Robot-Aided Prostate Cancer Diagnosis with Fiber Optic Sensing: A Validation Study on Phantoms and Ex-Vivo Tissues

Claudia Pecorella [1], Andrea Cirillo [1], Bruno Siciliano [1], Antonio Iele [2], Armando Ricciardi [2], Marco Consales [2], Andrea Cusano [2], Marco Capece [3,*], Giuseppe Celentano [3], Roberto La Rocca [3], Vincenzo Mirone [3] and Fanny Ficuciello [1]

[1] Department of Electrical Engineering and Information Technology, University of Naples Federico II, Via Claudio 21, 80125 Naples, Italy; claudia.pecorella@unina.it (C.P.); andrea.cirillo1987@gmail.com (A.C.); siciliano@unina.it (B.S.); fanny.ficuciello@unina.it (F.F.)

[2] Department of Engineer, University of Sannio, Via Traiano 3, 82100 Benevento, Italy; a.iele@unisannio.it (A.I.); aricciardi@unisannio.it (A.R.); consales@unisannio.it (M.C.); acusano@unisannio.it (A.C.)

[3] Department of Neuroscience, Reproductive and Odontostomatological Sciences University of Naples, Federico II, 80131 Naples, Italy; dr.giuseppecelentano@gmail.com (G.C.); robertolarocca87@gmail.com (R.L.R.); mirone@unina.it (V.M.)

* Correspondence: drmarcocapece@gmail.com

Abstract: Despite technological progress in instrumental diagnostic investigations of the last decade, prostate cancer remains one of the most frequent malignant tumors and the second leading cause of cancer death among men. Although prostate biopsy remains the reference among all diagnosis procedures, it still exposes patients to the risk of developing complications. In this paper, the authors present a novel robotic system for prostate cancer diagnosis aimed at improving the current diagnostic procedures and reducing their undesired effects. The purpose of this work is to validate the proposed methodology by considering experimental analysis on both phantom and ex-vivo prostate tissues.

Keywords: prostate cancer; PSA; fiber optic sensing; prostate biopsy; robot

1. Introduction

Prostate cancer represents the most common malignancy in men, accounting for estimated 164,690 new cases in the United States in 2018. According to the latest statistical report, prostate cancer still represents the second most common cause of death in men (9% of all cancer deaths), with an incremental trend due to the increasing life expectancy. Considering its high prevalence, extreme attention should be paid to the impact of the sanitary costs arising from the diagnostic and therapeutic procedures. While considering such a strong epidemiological implication, diagnostic procedures to detect this tumor have not undergone any significant developments in recent decades. Although finger palpation, known as the digital rectal examination (DRE), represents the common clinical maneuver for detecting prostate cancer, the outcome depends on the surgeon's experience. Therefore, the histological diagnosis after ultrasound-guided (USG) needle biopsy remains the only viable and accurate procedure. It should be emphasized that performing a prostate biopsy exposes the patients to the risk of developing complications that may affect their general condition. Furthermore, the rate of complications increases in the case of patients who need a large number of tissue samples or a re-do biopsy because prostate cancer is suspected.

Despite technological progress in instrumental diagnostic procedures, prostate biopsy still has a high risk of false negative results. Thus, even though needle biopsy remains the gold standard procedure for prostate cancer diagnosis, the efficacy of this technique remains controversial. During the last decade, numerous studies have been conducted to estimate and improve the actual detection rate. Several authors suggested that in order to increase the detection rate, the number of core sampling should be higher, e.g., 12-cores sampling or 20-cores sampling for each procedure, increasing the potential for side effects

of the procedure [1,2]. Despite the effort spent evaluating new clinical protocols, a false negative rate of around 30% prevails. Multiparametric magnetic resonance (mpMRI) of the prostate has been identified as a test that could reduce these diagnostic errors. However, the usefulness of mpMRI can vary depending on the population being studied, the execution of the MRI itself, the experience of the radiologist, on whether additional biomarkers are considered, and whether the mpMRI-targeted biopsy is carried out alone or in addition to systematic biopsy [3,4].

Considering this, new technologies are desirable to increase the level of accuracy of the prostatic core sampling. The use of a robotic system can improve the performance of a prostate biopsy, even overcoming the variability due to the manual skills of the operators. The aim of this paper is to evaluate and provide confirmation of the effectiveness of the initial part of the whole BARTOLO project (Bioptic Advanced Robotic Technologies in OncoLogy). In particular, the system analyzed here is represented by a fiber optics-based sensor installed on a commercial robotized system. Preliminary validation of this system on both phantom prostate tissues and real ex vivo prostate models is necessary and important in order to assess the performance of the sensor device and the robot control algorithms before proceeding with their integration into the whole robotized system.

2. Materials and Methods

BARTOLO is a project dedicated to the design of a new semi-controlled platform able to perform: (a) The prostate examination based on the DRE procedure along the different organ areas, evaluating the prostate tissue, i.e., cancer presence and its severity; (b) A real-time superimposition of the mpMRI images on trans-rectal ultrasound (TRUS) images; (c) An USG-biopsy on the suspected tissues if needed, to improve the precision of current diagnostic procedures and reduce complications due to the effects of the needle biopsy. In this paper, the authors will focus on the first step of this entire project. The final robotic system will be composed of:

- A robotic arm for transrectal applications, which simultaneously manages the movement of the triplane endocavitary ultrasound probe necessary to guide the execution of the biopsy sampling and the needle;
- An image fusion software, which integrates the preoperative MRI and the real-time ultrasound imaging, providing a three-dimensional model on which the targets can be precisely programmed;
- An autonomous control system, which uses the results of the image processing software to plan and control the motion of the needle and the probe;
- An optical fiber sensor, which can detect information related to the stiffness of the tissue from the analysis of the organ and transmit it to a database.

In detail, the 6-Degree of Freedom (DoF) Robotic Arm (Figure 1 for the CAD model) has been designed, focusing on the specific workspace requested to perform the diagnostic procedure on a real patient (see Figure 2). The robot allows the movement of the ultrasound probe and the pose regulation of the needle into the patient's anus once in contact with the prostate organ. At the robot wrist, a 6-axis force sensor is installed. The sensor is used to detect the interaction forces between the robot and the patient, to increase safety during the analysis, and to hand-guide the manipulator by the expert operator to bring the diagnostic instruments in contact with the rectum walls. The robot is constituted by a 4-DoFs rigid base connected to the ultrasound probe and the biopsy needle via a passive deformable element which introduces passive compliance resulting in two extra passive degrees of freedom in the robot kinematics. This passive compliance allows accommodating voluntary/involuntary movements of the patient compared with the robot actions, minimizing the interaction forces at the contact.
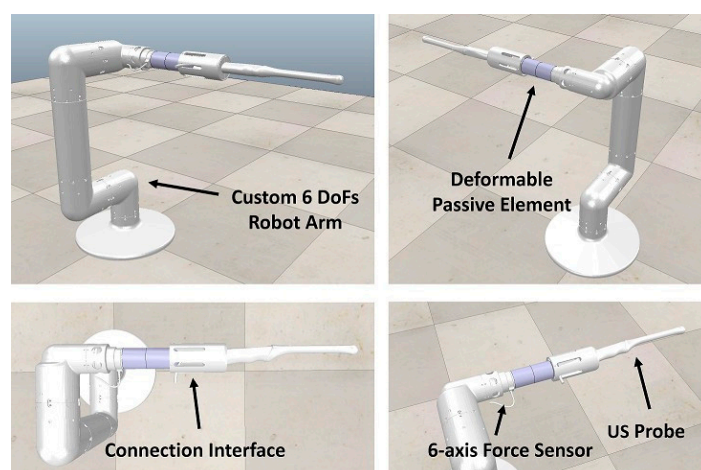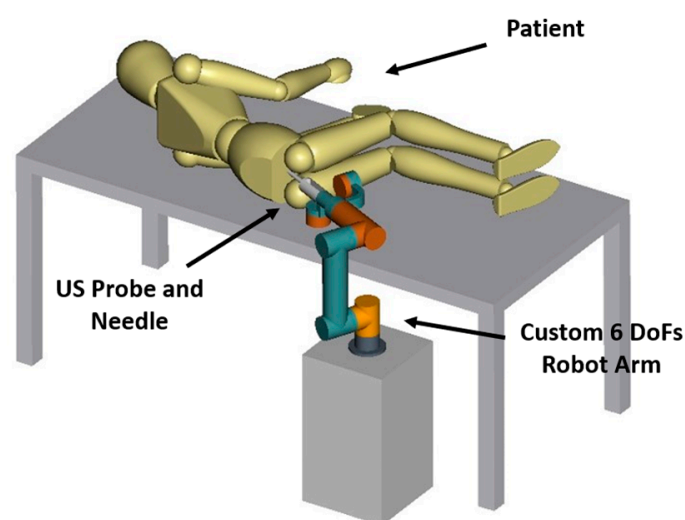
Figure 1. Custom 6-DoFs Robotic System.

Figure 2. Robotized Diagnostic Procedure Setup.

Significantly, few robot-aided biopsy procedures have been developed thus far; however, with the BARTOLO system, it is possible to automatize steps that are manually performed by clinicians, whose results are hence dependent on the clinicians' experience [5,6].

The final automatic procedure can be summarized as follow: (a) the robotic arm will be manually moved by the operator until the ultrasound probe tip enters into contact with the patient's anus, which will be the reference point of the examination; (b) the ultrasound probe will be inserted into the anus until the tip reaches initial position with respect to the prostate tissue; (c) from the fusion of the ultrasound probe images and the MRI images, the target will be detected, and the fiber optics-based force sensor will be brought on it; (d) the latter palpates the prostate tissue in the surroundings of the target point, and the acquired data will be used to estimate the elasticity of the tissue. The procedure can be repeated on several prostate areas to find suspicious tissues. If a region is classified as potentially malicious, the robotic system will be activated for tissue sampling.

A core element of the diagnostic system is represented by the highly accurate fiber optic-based force sensor. The latter is used to determine the morpho-functional characteristics of the prostate tissue. The analysis is based on a differential diagnostic approach carried out evaluating the tissue characteristics, i.e., elasticity, in different areas of the prostate.

Few works in the medical fields have demonstrated that, by analyzing the prostate tissue response through tensile or indentation tests, it is possible to determine the presence

of cancer and its severity focusing on the tissue rigidity/elasticity level. In the last decade, different studies have shown the effectiveness of the cancer diagnostic approaches based on the analysis of the mechanical conformation of the prostate. However, at the same time, they highlighted how the discrimination between malignant and healthy tissue could be made only with very accurate measurement systems. In fact, in the first stages of the disease, the tissues respond with minimal differences, e.g., 30 kPa for healthy prostates versus 50 kPa for malignant ones [7–10].

As previously mentioned, one of the main objectives of the project is the design and development of an automated framework for prostate analysis aimed to improve the efficiency and reliability of modern techniques for prostate cancer diagnosis. The first step is a setup to perform (a) analysis on prostate-like phantom tissue and (b) ex vivo analysis on real prostate organs obtained following radical prostatectomy surgery [11–13]. The mentioned analysis allows us to validate the performance of the sensor, of the control algorithms, and of the proposed diagnostic procedure.

The experimental setup shown in Figure 3a is composed of the following elements:

- A commercial 7-DoF Robotic Arm, i.e., KUKA LBR Med 7,
- The fiber optics-based force sensor [14,15],
- The prostate tissue, i.e., prostate-like phantom tissue or real prostate organ obtained from a radical prostatectomy surgery.
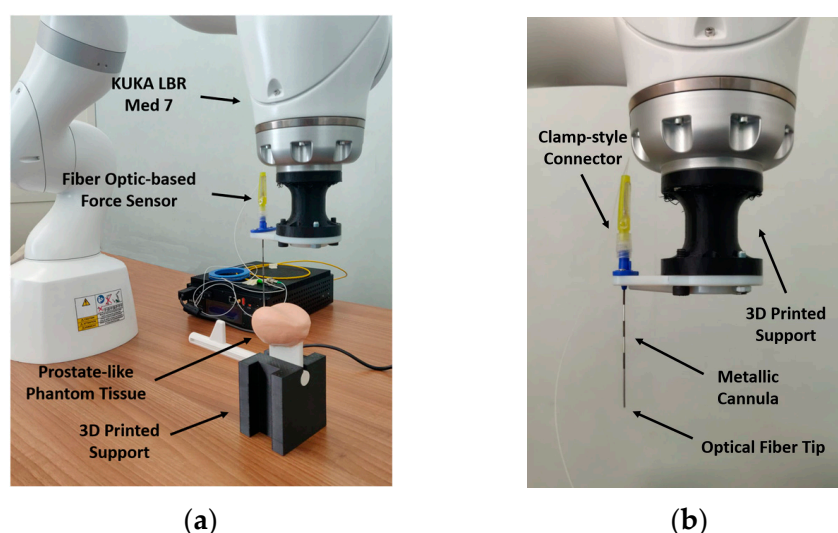

(**a**)   (**b**)

Figure 3. Experimental Setup. (**a**) Setup overview, (**b**) Fiber Optics-based force sensor.

The idea underlying the framework for ex vivo prostate tissues analysis is to exploit the fiber optics-based sensor to inspect different points on the prostate through indentation actions. It is possible to estimate the elasticity of the material by knowing how many millimeters the force sensor sinks into the prostate tissue and measuring the force exerted on it during the indentation [16]. The harder the tissue, the higher the suspicion of a cancerous area. The acquired data on various points are used to distinguish between the physiological and pathological areas of the tissue. According to the 12-core based needle biopsy procedure [1], the prostate under analysis is divided into 10 areas, and 12 main indentation cores are considered (Figure 4). In this way, it is possible to distinguish: four Base areas, four Middle areas, and two Apex areas with two inspection points for each one.
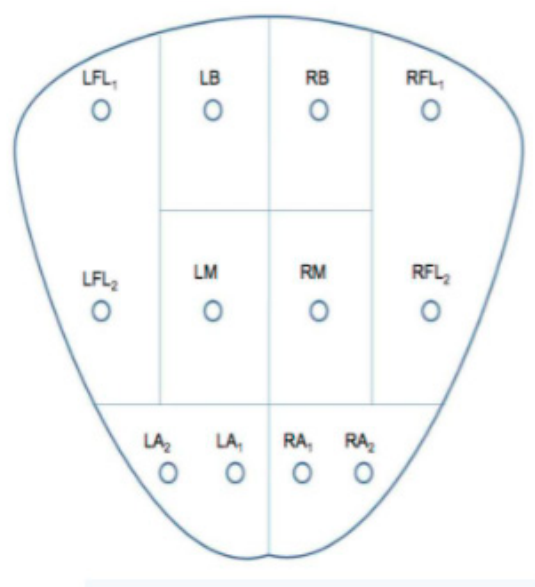
Figure 4. Prostate 12-cores analysis.

3. Results

The proposed approach has been validated by acquiring data from two different tests. First, tests on prostate-like phantom models have been performed in order to prove the approach's effectiveness and to demonstrate the validity of the results. Subsequently, preliminary tests on real prostate tissues obtained from a radical prostatectomy surgery have been conducted to confirm the feasibility of prostate-like phantoms. In both scenarios, sensor force data have been used to determine the induration of the tissues undergoing the analysis. The authors are keen to emphasize that the tests on real prostate organs reported in this paper are only preliminary, and a deeper experimental campaign will be carried out to determine the value of the approach from a clinical point of view.

3.1. Prostate-like Phantom Tissue Analysis

This section describes the experiments performed on prostate-like phantom tissues. The goal of this analysis is to show the effectiveness of the proposed methodology by focusing on the capacity of the sensory system to classify soft and hard areas by exploiting force measures. In particular, the tissues under analysis are: one soft phantom tissue, reflecting normal parenchyma that will be named "physiological" (Figure 5a), and one phantom tissue with hardening, reflecting cancerous parenchyma, that will be named "pathological" (Figure 5b). As Figure 5b shows, the pathological phantom tissue presents a large hard area, more rigid and irregular, well exposed over the tissue surface as in a severe cancer stage. The physiological phantom model, on the other hand, has a more homogeneous conformation. Figure 5 also reports the 12-core-based map, overlapped to the phantom tissues, used for the inspection analysis. The four red points that determine the perimeter of the area undergoing the analysis have been manually acquired through the robot with manual guidance operations. The 12 inspection points have been generated through the software tool previously mentioned. From Figure 5b, it can be discerned that the third point of the inspection map falls on the hard area of the pathological phantom tissue, whereas the second and fourth lie on irregular surfaces of the phantom close to the hard area. From the previous discussion, it is expected that points 2, 3, and 4 shall behave differently from the other points.
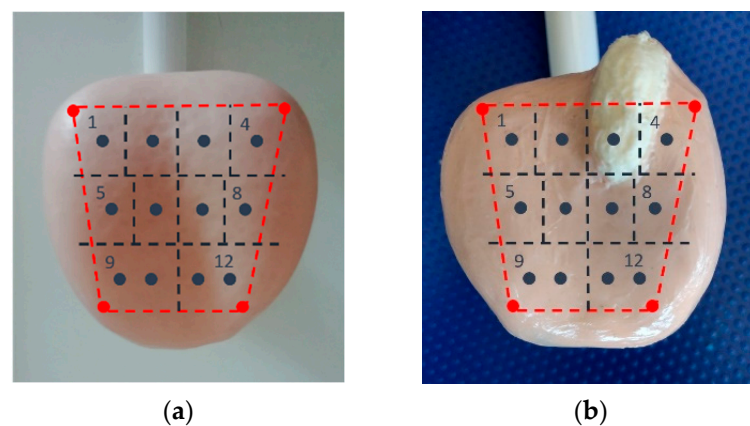
Figure 5. Prostate-like phantom Tissues. (**a**): physiological phantom prostate model shows healthy phantom tissues; (**b**): pathological phantom prostate model shows an ill phantom tissue.

Figure 6 reports the results obtained by a typical experiment on the phantom tissues, i.e., the force measured with the fiber optic-based sensor for the physiological phantom (Figure 6a) and the pathological phantom (Figure 6b) case. The experiment results have shown 12 force peaks corresponding to the 12 cores considered in the inspection procedure. Focusing on single force peaks and referring to the inspection procedure described before, two macrophages can be detected. During the first, the tissue surface is detected through the admittance control algorithm. In the specific experiments, the target force has been chosen as f_{dz} = 0.2 N. During this phase, the robot is forced to move the controller to reach the organ surface until the robot tips enter into a steady-state, maintaining the reached position 2 s. During the second phase, the inspection procedure is executed. The robot is position-controlled in order to indent the organ surface for 2 mm. During the indentation, the amplitude of the measured force gets higher according to the tissue mechanical characteristics, i.e., elasticity.
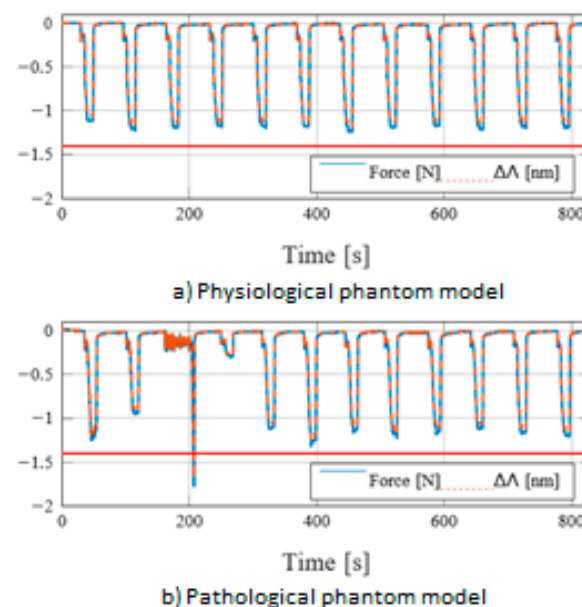

Figure 6. Tests on phantom prostate models: Experimental Results.

From Figure 6a, it can be noticed that, for the healthy prostate, the force peaks for the 12 inspection points are similar enough to demonstrate tissue uniformity. The maximum recorded force amplitude is around 1.2 N. Considering the analysis made on the pathological phantom prostate (Figure 6b), it is evident the different behavior registered on

the point 3, where the measured force is higher than the one obtained both on the healthy phantom and the other points of the ill phantom. In particular, the registered force reaches the safety threshold of 1.8 N set to stop the indentation procedure in order to avoid possible damage to the sensor or the organ. Moreover, the higher stiffness of the induration area influences the dynamics of the admittance control, which responds with a more unstable behavior. Regarding the points 2 and 4, the measured forces are lower than the others. In fact, for point 4, an amplitude of 0.35 N is registered. This behavior is associated with the slope immediately close to the hardening of the model, which does not allow a stable and perpendicular contact between the sensor and the organ. The high measured force, together with the behavior obtained in the points adjacent to the induration area, gives a clear indication of the state of the analyzed tissue.

By comparing the results obtained with the two experiments, a threshold of 1.4 N may be considered a valid criterion to distinguish the physiological state of the phantom prostates.

3.2. Real Prostate Tissue Analysis

The proposed methodology has also been validated on real prostate organs obtained from radical prostatectomy surgeries. In this section, the results of a typical test are described. Currently, the tests belong to preliminary analysis, and extensive experimentation on ex vivo prostates is ongoing.

Figure 7 shows the prostate under analysis and the 12-core map considered in the presented test. The yellow box represents the a priori information about the cancerous area detected through a mpMRI study. In Figure 8, the force profile acquired during the test is reported. The force profile presents a lower mean value compared to the experiments carried out on the phantom tissues. This behavior is due to the difference in stiffness between the phantom and the real prostate models (the phantom tissue is stiffer than the real prostate). Given the lower forces exerted during the contact, a lower target force for the admittance control has been chosen, i.e., $f_{dz} = 0.05$ N. In the mentioned conditions, the last three analyzed points, which correspond to the tumoral area based on the mpMRI images, show a higher force peak than the others. The differences in the recorded forces give a clear indication of the presence of a pathological area that, in this specific test, can be detected by thresholding the forces with the value $f_{thr} = -0.35$ N. This experiment has been repeated four times on different real prostates. Furthermore, the tests on real organs prove the effectiveness of the proposed approach as the results have been confirmed by histological analysis.
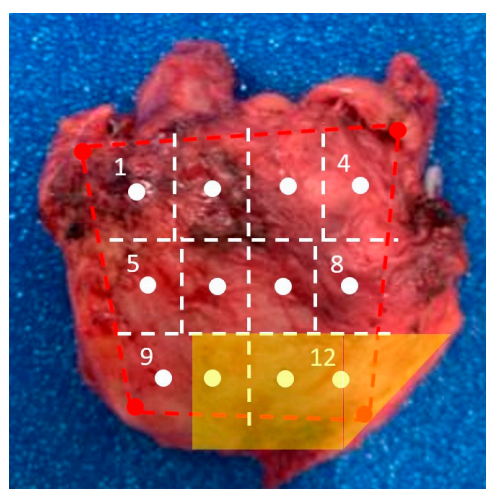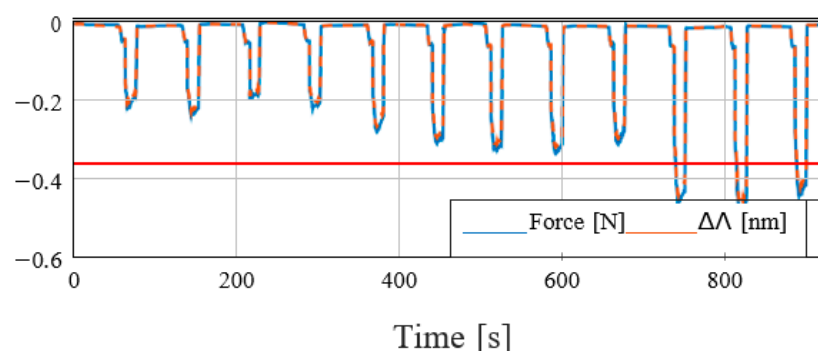

Figure 7. Real Prostate Tissue.

Figure 8. Tests on Real Prostate Tissues: Experimental Results.

4. Limitation

This paper is a pilot study and faces some limitations. The major limitation is that the experiments on actual prostates are very limited in number; thus, a proper "cut-off" value of the exerted forces cannot be calculated. The second limitation is due to the relativity of the response forces that should be tested on many pathological phantom models to assess the reliability of the technique regardless of the location or the size of the hardening.

5. Discussion and Conclusions

Recently, the literature has been moving towards a less invasive and more efficacious way of diagnosing prostate cancer. Indeed, Tafuri et al. have already stated that systematic biopsy can be omitted in patients with high suspicion of prostate cancer at mpMRI (PIRADS 5) in favor of a targeted biopsy [17].

In this work, the authors presented a novel robotic system for prostate cancer diagnosis with the aim to improve the current diagnostic procedures using a fiber optics-based sensor that can inspect different organ points through indentation. Other prototypes of prostate biopsy robots have been developed and validated in the past; however, none of them have used such technology to improve prostate cancer detection. Maris et al. developed a robot able to perform a targeted biopsy through ultrasound guidance and magnetic resonance images fusion, and needle positioning [18].

Our robotic system makes it possible to reproduce, in an autonomous manner, a prostate examination based on the classical DRE procedure along different organ areas. By evaluating the tissue's mechanical response exploiting the force measures provided by the fiber optics-based sensor, it is possible to detect a valid criterion to distinguish the pathological tissues from the physiological ones on phantom prostate models. In the present study, the authors have also assessed the reproducibility of the technique on ex vivo real prostate. However, as shown above, the authors cannot distinguish different physiological and pathological aspects of prostatic tissue because only the prostate tissues affected by adenocarcinoma have been tested. Future studies will focus on determining a cut-off response value for prostate cancer tissues to differentiate between benign and malignant areas. This will be the primary outcome of these studies. In the literature, only a few robot-aided biopsies have been developed over the last decades; however, none have changed the actual clinical procedure. The BARTOLO system could represent a valid and effective solution to be followed in the future.

Institutional Review Board Statement: Not applicable.

Informed Consent Statement: Not applicable.

Conflicts of Interest: The authors declare no conflict of interest.

References

1. Serefoglu, E.C.; Altinova, S.; Ugras, N.S.; Akincioglu, E.; Asil, E.; Balbay, M.D. How reliable is 12-core prostate biopsy procedure in the detection of prostate cancer? *Can. Urol. Assoc. J.* **2013**, *7*, E293–E298. [CrossRef] [PubMed]

2. Ravery, V.; Dominique, S.; Panhard, X.; Toublanc, M.; Boccon-Gibod, L. The 20-core prostate biopsy protocol–a new gold standard? *J. Urol.* **2008**, *179*, 504–507. [CrossRef] [PubMed]

3. Stanzione, A.; Creta, M.; Imbriaco, M.; La Rocca, R.; Capece, M.; Esposito, F.; Imbimbo, C.; Fusco, F.; Celentano, G.; Napolitano, L.; et al. Attitudes and perceptions towards multiparametric magnetic resonance imaging of the prostate: A national survey among Italian urologists. *Arch. Ital. Urol. Androl.* **2020**, *17*, 92. [CrossRef] [PubMed]

4. Pepe, P.; Pepe, G.; Pepe, L.; Garufi, A.; Priolo, G.D.; Pennisi, M. Cost-effectiveness of Multiparametric MRI in 800 Men Submitted to Repeat Prostate Biopsy: Results of a Public Health Model. *Anticancer. Res.* **2018**, *38*, 2395–2398. [CrossRef] [PubMed]

5. Ahn, B.; Kim, Y.; Oh, C.K.; Kim, J. Robotic palpation and mechanical property characterization for abnormal tissue localization. *Med. Biol. Eng. Comput.* **2012**, *50*, 961–971. [CrossRef] [PubMed]

6. Ahn, B.; Lee, H.; Kim, Y.; Kim, J. Robotic system with sweeping palpation and needle biopsy for prostate cancer diagnosis. *Int. J. Med. Robot.* **2014**, *10*, 356–367. [CrossRef] [PubMed]

7. Tafuri, A.; Ditonno, F.; Panunzio, A.; Gozzo, A.; Porcaro, A.B.; Verratti, V.; Cerruto, M.A.; Antonelli, A. Prostatic Inflammation in Prostate Cancer: Protective Effect or Risk Factor? *Uro* **2021**, *1*, 54–59. [CrossRef]

8. Peng, Q.; Omata, S.; Peehl, D.M.; Constantinou, C.E. Stiffness mapping prostate biopsy samples using a tactile sensor. In Proceedings of the 2011 Annual International Conference of the IEEE Engineering in Medicine and Biology Society, Boston, MA, USA, 30 August–3 September 2011; pp. 8515–8518. [CrossRef]

9. Kelly, N.P.; Flood, H.D.; Hoey, D.A.; Kiely, P.A.; Giri, S.K.; Coffey, J.C.; Walsh, M.T. Direct mechanical characterization of prostate tissue-a systematic review. *Prostate.* **2019**, *79*, 115–125. [CrossRef] [PubMed]

10. Zein, S.; Ghomsheh, F.T.; Jamshidian, H. Evaluation of Artificial Tactile Sense in Mass Detection in Silicone Phantom for the Diagnosis of Prostate Tumor. *Bull. Exp. Biol. Med.* **2020**, *169*, 497–503. [CrossRef] [PubMed]

11. Cirillo, A.; Ficuciello, F.; Natale, C.; Pirozzi, P.; Villani, L. A Conformable Force/Tactile Skin for Physical Human–Robot Interaction. *IEEE Robot. Autom. Lett.* **2016**, *1*, 41–48. [CrossRef]

12. Maciejewski, A.A.; Klein, C.A. Numerical Filtering for the Operation of Robotic Manipulators through Kinematically Singular Configurations. *J. Robot. Syst.* **1988**, *5*, 527–552. [CrossRef]

13. Carotenuto, B.; Micco, A.; Ricciardi, A.; Amorizzo, E.; Mercieri, M.; Cutolo, A.; Cusano, A. Optical Guidance Systems for Epidural Space Identification. *IEEE J. Sel. Top. Quantum Electron.* **2017**, *23*, 371–379. [CrossRef]

14. Iele, A.; Ricciardi, A.; Pecorella, C. Miniaturized optical fiber probe for prostate cancer screening. *Biomed. Opt. Expressthis* **2021**, *12*, 5691–5703. [CrossRef] [PubMed]

15. Carotenuto, B.; Ricciardi, A.; Micco, A.; Amorizzo, E.; Mercieri, M.; Cutolo, A.; Cusano, A. Smart Optical Catheters for Epidurals. *Sensors* **2018**, *18*, 2101. [CrossRef] [PubMed]

16. Hill, K.O.; Meltz, G. Fiber Bragg grating technology fundamentals and overview. *J. Lightw. Tech.* **1997**, *15*, 1263–1276. [CrossRef]

17. Tafuri, A.; Iwata, A.; Shakir, A.; Iwata, T.; Gupta, C.; Sali, A.; Sugano, D.; Mahdi, A.S.; Cacciamani, G.E.; Kaneko, M.; et al. Systematic Biopsy of the Prostate can Be Omitted in Men with PI-RADS™ 5 and Prostate Specific Antigen Density Greater than 15%. *J. Urol.* **2021**, *206*, 289–297. [CrossRef] [PubMed]

18. Maris, B.; Tenga, C.; Vicario, R.; Palladino, L.; Murr, N.; De Piccoli, M.; Calanca, A.; Puliatti, S.; Micali, S.; Tafuri, A.; et al. Toward autonomous robotic prostate biopsy: A pilot study. *Int. J. Comput. Assist. Radiol. Surg.* **2021**, *16*, 1393–1401. [CrossRef] [PubMed]